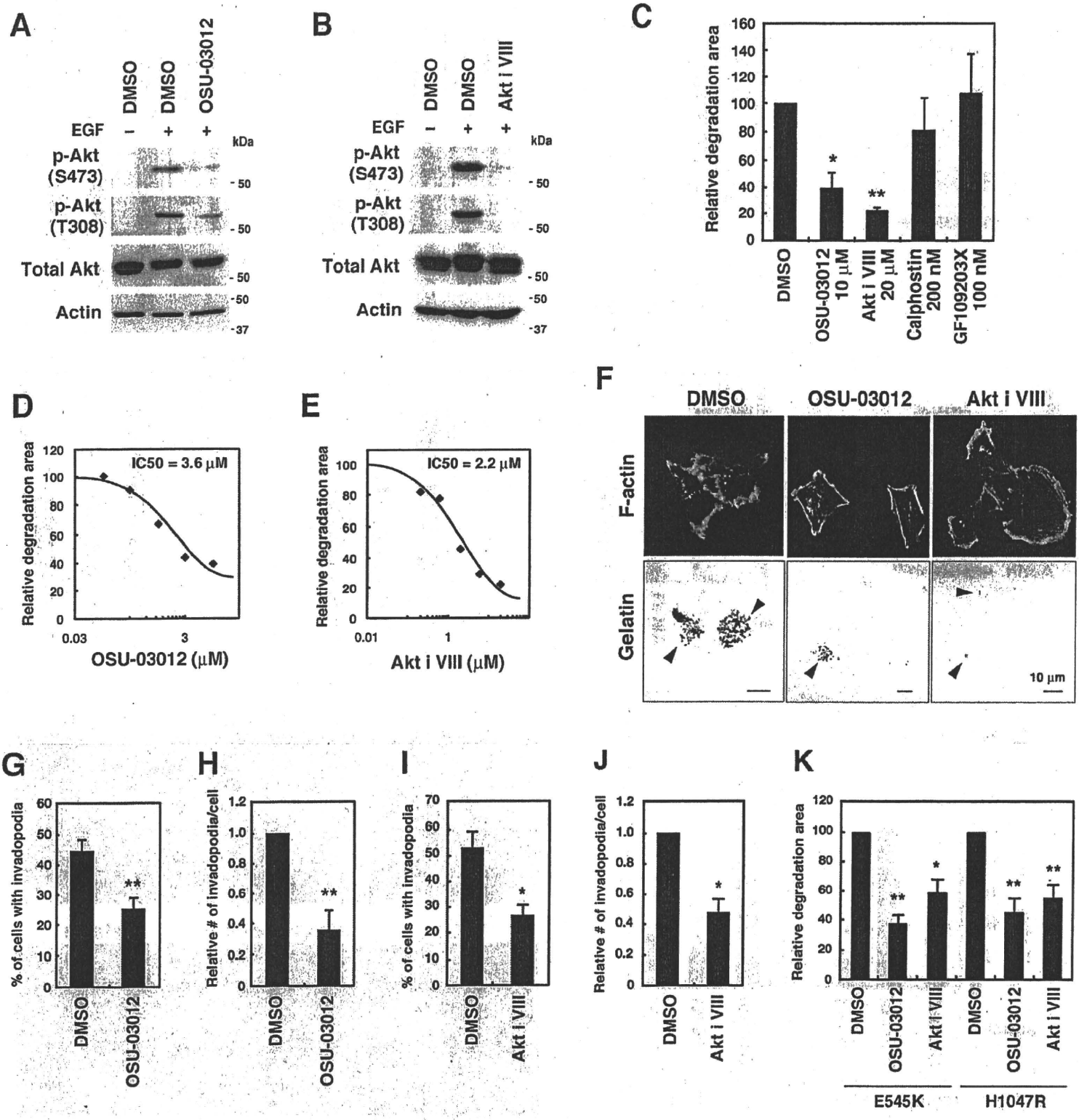

Yamaguchi et al. Fig. 6

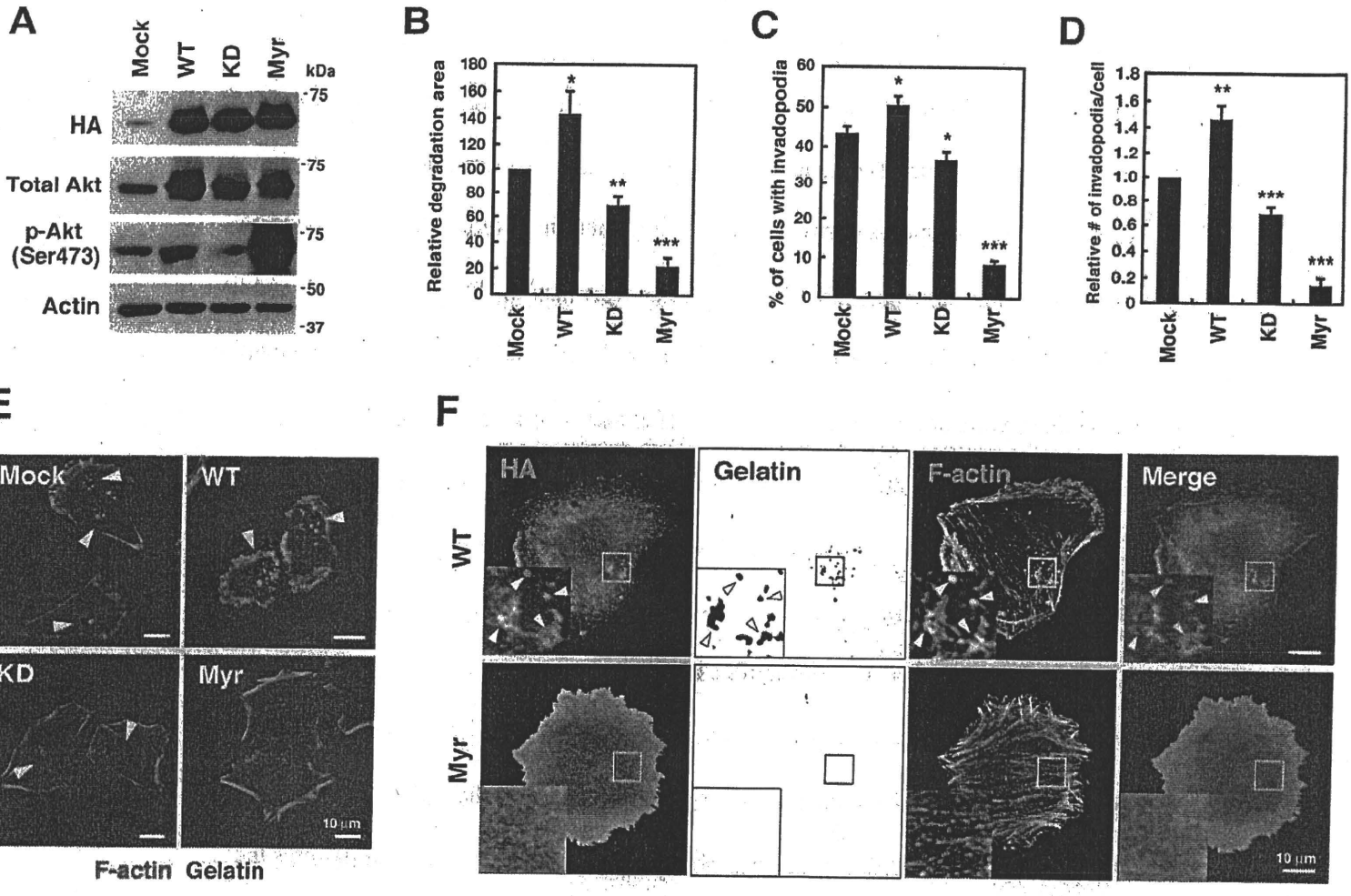

Yamaguchi et al. Fig. 7

Supplementary Figure Legends

Figure S1. PI3K activity is required for invadopodia formation in MDA-MB-231 cells.

(A) MDA-MB-231 cells were cultured on fluorescent gelatin-coated coverslips for 7 h in the presence or absence of LY294002 (LY) or wortmannin (WM) and stained for cortactin and F-actin to visualize invadopodia. Arrowheads denote degradation sites on the gelatin matrix. (B) Quantification of the gelatin degradation activity is shown. (C and D) Dose-response curves of gelatin degradation obtained in the presence of increasing concentrations of LY294002 (C) or wortmannin (D) are shown. (E and F) The percentage of cells with invadopodia (E) and the relative number of invadopodia per cell (F) were determined. Data in (B), (E), and (F) are represented as mean (+SEM) of 4 independent determinations. * $p < 0.02$, and ** $p < 0.005$ by Student's *t*-tests. (G) Cells stably expressing GFP-actin were cultured on gelatin-coated glass-bottom dishes and observed using time-lapse fluorescent microscopy. Representative images of a cell before and 1 min after LY294002 treatment are shown. Insets are magnified images of the boxed regions. Arrowheads denote invadopodia that were degraded after LY294002 treatment. (H) Quantification of the fluorescence intensity at the invadopodia in GFP-actin expressing cells is shown. Arrowhead denotes the time point of DMSO or LY294002 addition. Data are represented as mean (±SD) of 7 and 6 invadopodia for DMSO- and LY294002-treated cells, respectively. * $p < 0.001$ by Student's *t*-tests.

Figure S2. The expression levels of GFP-Akt1-PH and localization of GFP in MDA-MB-231 cells.

(A) The expression levels of GFP-Akt1-PH were determined in transiently and stably transfected MDA-MB-231 cells. Relative fluorescence intensity of the GFP-Akt1-PH signals was calculated from microscopic images. Data are mean (+SEM) of 38 transient cells and 35 stable cells analyzed. (B) MDA-MB-231 cells stably expressing a GFP construct were cultured on fluorescent gelatin-coated coverslips, stained for F-actin, and observed by confocal microscopy.

Figure S3. RT-PCR analysis of the expression of PI3K and Akt isoforms in MDA-MB-231 cells.

(A) The expression of PI3K isoforms was determined by semi-quantitative RT-PCR analysis. The expression of class I p110α, p110β, p110δ; class II C2α, C2β; and class III Vps34 was detected, while expression of class I p110γ and class II C2γ was not detected. This is consistent with the result obtained by real-time quantitative PCR analysis with a different set of primer pairs for the PI3K isoforms (shown in Fig. 2A). (B) The expression of Akt isoforms was determined by real-time quantitative PCR analysis. All 3 Akt isoforms were expressed in MDA-MB-231 cells. Data are mean (+SEM) of three independent experiments.

Figure S4. The function of p110α in invadopodia formation and localization of PDK1 and Akt at invadopodia in human breast cancer cells.

(A) MDA-MB-231 cells were transfected with three different siRNAs that target distinct regions of the *PIK3CA* gene for 48 h, and the expression of p110α was examined by immunoblotting. (B) MDA-MB-231 cells transfected with the p110α siRNAs were cultured on fluorescent gelatin-coated coverslips for 7 h, and the degradation area of gelatin was quantified. (C) BT-549 cells transfected with control

or p110α siRNA were cultured on fluorescent gelatin-coated coverslips for 7 h and stained for F-actin. (D) Gelatin degradation activity of BT549 cells transfected with control or p110α siRNA was quantified. (E) Expression of p110α in Hs578T cells expressing control or p110α shRNA was examined by immunoblotting. (F) Hs578T cells expressing control or p110α shRNA were cultured on fluorescent gelatin-coated coverslips for 16 h and stained for F-actin. (G) Gelatin degradation activity of Hs578T cells expressing control or p110α shRNA was quantified. (H) BT-549 and Hs578T cells were plated onto fluorescent gelatin-coated coverslips for 7 h and 16 h, respectively, in the absence or presence of 100 nM of PIK-75. The gelatin degradation areas were then quantified. (I) Representative images of BT549 and Hs578T cells treated with 100 nM of PIK-75 are shown. (J) BT549 cells plated onto fluorescent gelatin-coated coverslips for 16 h were stained with anti-Akt and anti-PDK1 antibody. Arrowheads denote accumulation of Akt and PDK1 signals at the gelatin degradation sites. Inserts in all images are magnified images of the boxed regions. Data in (B, H, and G) and (D) are mean (+SEM) of 4 and 6 independent determinations, respectively. * $p<0.01$, and ** $p<0.001$ by Student's *t*-tests.

Figure S5. The effects of expression of constitutively active Akt1 mutants on invadopodia formation.

(A) MDA-MB-231 cells stably expressing HA-tagged E17K and E40K Akt1 were analyzed by immunoblotting. (B) Cells stably expressing the Akt constructs were cultured on fluorescent gelatin-coated coverslips for 7 h and degraded areas on the gelatin matrix were quantified. Data are represented as mean (+SEM) of 4 independent determinations. * $p < 0.001$ by Student's t-tests.

Video 1. Time-lapse imaging of invadopodia in MDA-MB-231 cells expressing GFP-actin.

MDA-MB-231 cells stably expressing GFP-actin were cultured on gelatin-coated glass-bottomed dishes and treated with 20 μM LY294002. Cells were imaged every 1 min by epifluorescence time-lapse microscopy. The play rate was 6 frames/s, and the cells were tracked for a total of 30 min. Corresponding still images are shown in Supplementary Figure S1G.

Video 2. *Time-lapse imaging of invadopodia in MDA-MB-231 cells expressing Venus-cortactin.*

MDA-MB-231 cells stably expressing Venus-cortactin were cultured on gelatin-coated glass-bottom dishes and treated with 20 μM LY294002. Cells were imaged every 1 min by epifluorescence time-lapse microscopy. The play rate was 6 frames/s, and the cells were tracked for a total of 16 min. Invadopodia enriched with cortactin immediately disassembled after addition of LY294002.

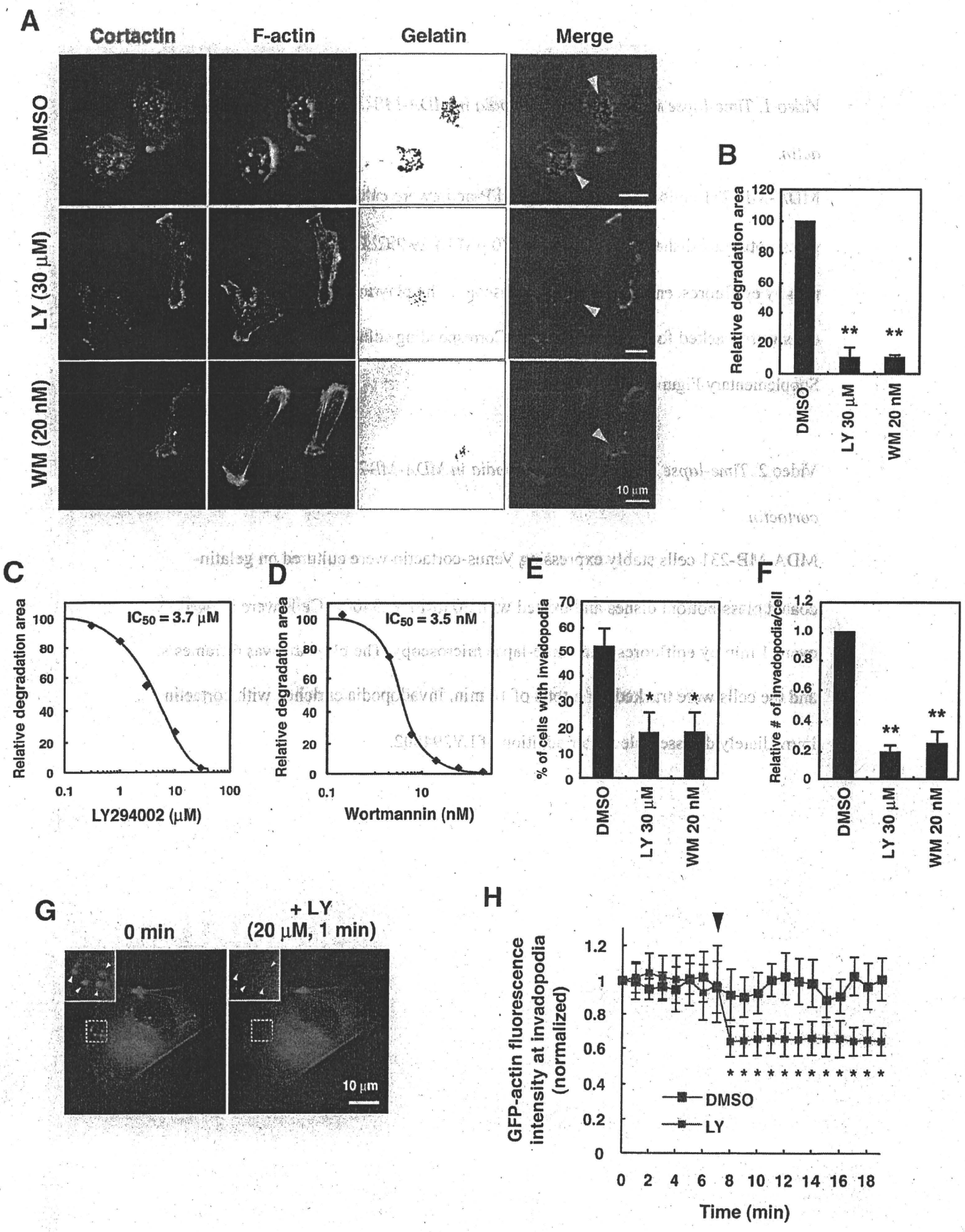

Yamaguchi et al. Fig. S1

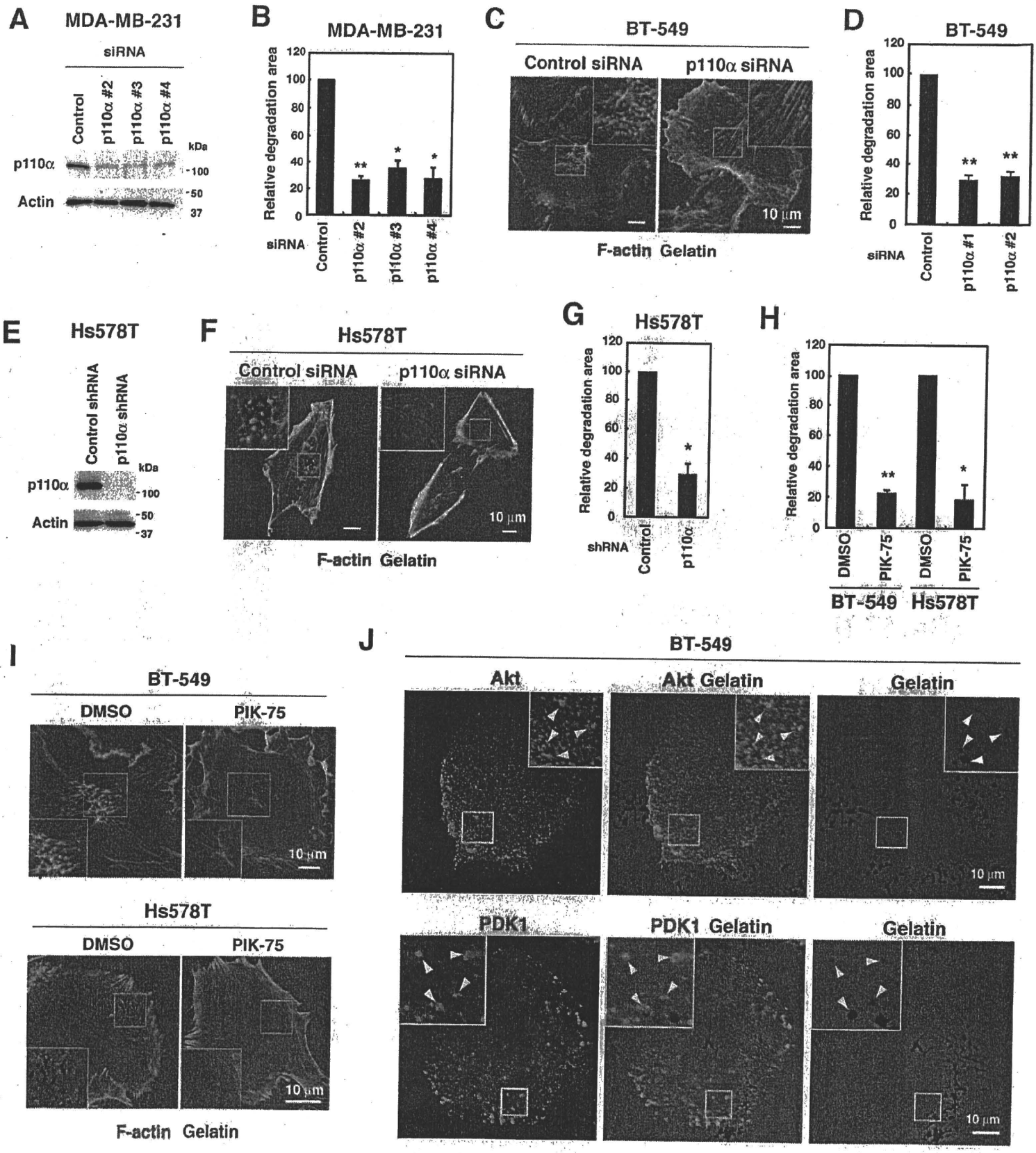

Yamaguchi et al. Fig. S4

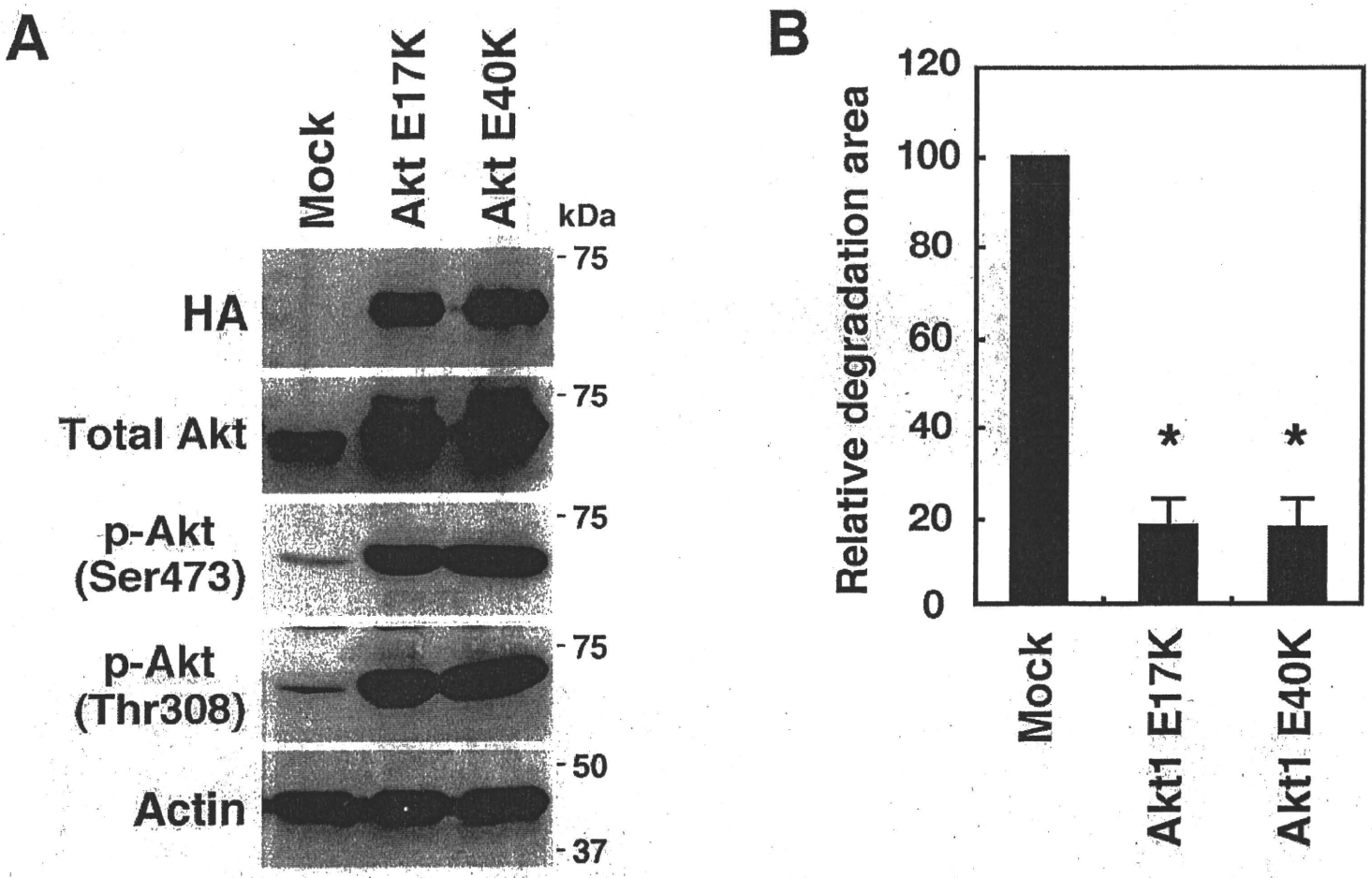

Yamaguchi et al. Fig. S5

Supplementary Table S1: List of siRNAs used in this study

Gene symbol	Gene ID	Stealth RNAi
PIK3CA	5290	#1 Stealth Select RNAi HSS108004
		#2 Stealth Select RNAi HSS108005
		#3 GCGTTTCTGCTTTGGGACAACCATA
		#4 CAGGCAAAGACCGATTGCATAGGAA
		#5 GCAAACAGGGTTTGATAGCACTTAA
PIK3CB	5291	Stealth Select RNAi HSS108007
PIK3CD	5293	Stealth Select RNAi HSS108013
PIK3C2A	5286	Stealth Select RNAi HSS107992
PIK3C2B	5287	Stealth Select RNAi HSS107996
PIK3C3	5289	Stealth Select RNAi HSS108003
PDK1	5170	#1 Stealth Select RNAi HSS107791
		#2 Stealth Select RNAi HSS182203
Akt1	207	#1, 2 Validated Stealth DuoPak 12935-001
Akt2	208	#1, 2 Validated Stealth DuoPak 12937-40
Akt3	10000	#1 Stealth Select RNAi HSS115177
		#2 Stealth Select RNAi HSS115178
Control		Negative Control Medium GC Duplex #2

Supplementary Table S2: List of primer pairs used for PCR analyses

Gene symbol	Gene ID	Sequence 5'-3'
For real-time quantitative PCR		
PIK3CA	5290	TGGATGCTCTACAGGGCTTT
		GTCTGGGTTCTCCCAATTCA
PIK3CB	5291	GCATTAAAAGGGAGCGAGTG
		CATGCCGTCGTAAAATCAGA
PIK3CD	5293	CTGGCTGAAGTCCAAGAACC
		CTCGGATCATGATGTTGTCG
PIK3CG	5294	ATACCATGATAGCGCCCTTG
		AATCACAGCGAACCTCTGCT
PIK3C2A	5286	GAAAAACGAGGAATCCGACA
		CAGGGTTACTCCACCCAAGA
PIK3C2B	5287	TTCCCTAGTCGCTTCGTGAT
		CAGTGGGTGGAAGAAGGTGT
PIK3C2G	5288	TTCATCTCCCAGATGGCTCT
		AGTGGGGTCCGTACATTTTG
PIK3C3	5289	TCAGCCAAGCATTGTTGAAG
		TCCACTTTCGCGTTGTACTG
Akt1	207	TCTATGGCGCTGAGATTGTG
		CTTAATGTGCCCGTCCTTGT
Akt2	208	TATACCGCGACATCAAGCTG
		GGTCCCACAGAAGGTTTTCA
Akt3	10000	TGGACAAAGATGGCCACATA
		ACTGCTCGGCCATAGTCATT
PPIB (Cyclophilin B)	5479	TTCTAGAGGGCATGGAGGTG
		GCTTCTCCACCTCGATCTTG
For semi-quantitative RT-PCR		
PIK3CA	5290	GTCAATCGGTGACTGTGTGG
		TCCATCGTCTTTCACCATGA
PIK3CB	5291	GGGAAAGCTCATCGTAGCTG
		CTTGATCTTGCAGCATTCCA
PIK3CD	5293	CTGGTGCAGGTGCTCAAGTA
		TGAGAGCTCAGCTTGACGAA
PIK3CG	5294	GGAACACCGACCTCACAGTT
		GAAGCTGAACTTTGCCCTTG
PIK3C2A	5286	ACATCCGGAACCAACAAGAG
		TTCAGCTTGGGTGAGCTTTT
PIK3C2B	5287	GGCCATGAGTTGTTTGAGGT
		CATCATGGGTGTAGCACAGG
PIK3C2G	5288	CTCATTGGTGGCACCTACCT
		AGCCATCTGGGAGATGAATG
PIK3C3	5289	CTCACCAAAGCTCATCGACA
		GCTTGTGGTGTTTGCTCTCA
PPIB (Cyclophilin B)	5479	GCACAGGAGGAAAGAGCATC
		CTTCTCCACCTCGATCTTGC

Genes to Cells

Tyrosine phosphorylation of R3 subtype receptor-type protein tyrosine phosphatases and their complex formations with Grb2 or Fyn

Yoji Murata, Munemasa Mori, Takenori Kotani, Yana Supriatna, Hideki Okazawa, Shinya Kusakari, Yasuyuki Saito, Hiroshi Ohnishi and Takashi Matozaki*

Laboratory of Biosignal Sciences, Institute for Molecular and Cellular Regulation, Gunma University, 3-39-15 Showa-Machi, Maebashi, Gunma 371-8512, Japan

Post-translational modification of protein tyrosine phosphatases (PTPs) is implicated in functional modulation of these enzymes. Stomach cancer–associated protein tyrosine phosphatase-1 (SAP-1), as well as protein tyrosine phosphatase receptor type O (PTPRO) and vascular endothelial-protein tyrosine phosphatase (VE-PTP) are receptor-type PTPs (RPTPs), which belong to the R3 subtype RPTP family. Here, we have shown that the carboxyl (COOH)-terminal region of SAP-1 undergoes tyrosine phosphorylation by the treatment with a PTP inhibitor. Src family kinases are important for the tyrosine phosphorylation of SAP-1. Either Grb2 or Fyn, through their Src homology-2 domains, bound to the tyrosine-phosphorylated SAP-1. Moreover, both PTPRO and VE-PTP underwent tyrosine phosphorylation in their COOH-terminal regions. Tyrosine phosphorylation of VE-PTP or PTPRO also promoted their complex formations with Grb2 or Fyn. Forced expression of SAP-1, PTPRO or VE-PTP promoted cell spreading and lamellipodium formation of fibroblasts that expressed an activated form of Ras. In contrast, such effects of non-tyrosine-phosphorylated forms of these RPTPs were markedly smaller than those of wild-type RPTPs. Our results thus suggest that tyrosine phosphorylation of R3 subtype RPTPs promotes their complex formations with Grb2 or Fyn and thus participates in the regulation of cell morphology.

Introduction

Protein tyrosine phosphatases (PTPs) play important roles in regulation of various cell functions including cell proliferation, differentiation and migration through tyrosine dephosphorylation of their substrates (Alonso *et al.* 2004). Many of PTPs are regulated by post-translational modifications such as glycosylation, oxidation and phosphorylation (Alonso *et al.* 2004; den Hertog *et al.* 2008). Such modifications are implicated in regulation of multiple functions of PTPs. Indeed, phosphorylation of several PTPs at either serine or tyrosine residues is implicated in regulation of the catalytic activity, the intra-molecular conformation of PTPs or the interaction of PTPs with other signaling molecules (den Hertog *et al.* 2008). However, the detailed information regarding post-translational modifications of individual PTPs as well as their physiological roles remains limited.

Stomach cancer–associated protein tyrosine phosphatase-1 (SAP-1) [also known as protein tyrosine phosphatase receptor type H (PTPRH)] was originally identified as a PTP expressed in a human stomach cancer cell line (Matozaki *et al.* 1994). It is classified as a receptor-type PTP (RPTP) of the R3 subtype (Andersen *et al.* 2001), as are protein tyrosine phosphatase receptor type O (PTPRO) [also known as glomerular epithelial protein 1 (GLEPP1)] (Thomas *et al.* 1994; Wang *et al.* 2000), vascular endothelial-protein tyrosine phosphatase (VE-PTP) [also known as protein tyrosine phosphatase receptor type B (PTPRB) or PTPβ] (Krueger *et al.* 1990; Fachinger *et al.* 1999) and density-enhanced phosphatase-1 (DEP-1) (Östman *et al.* 1994; Kuramochi *et al.* 1996; Jallal *et al.* 1997). All of these PTPs share similar

Communicated by: Yoshimi Takai
**Correspondence*: matozaki@showa.gunma-u.ac.jp

DOI: 10.1111/j.1365-2443.2010.01398.x

structures, with a single catalytic domain in the cytoplasmic region and fibronectin type III–like domains in the extracellular region. We have recently demonstrated that expression of SAP-1 in mice is largely restricted to the gastrointestinal tract and it localizes to the microvilli of the brush border in gastrointestinal epithelial cells (Sadakata *et al.* 2009). Although the physiological function of SAP-1 *in vivo* remains unclear, SAP-1 ablation inhibited tumorigenesis in mice with a heterozygous mutation of the adenomatous polyposis coli gene, suggesting that SAP-1 potentially regulates intestinal tumorigenesis (Sadakata *et al.* 2009). PTPRO is specifically expressed in podocytes of the renal glomerulus (Thomas *et al.* 1994; Yang *et al.* 1996); in particular, it is localized at the apical surface of foot processes in the highly polarized visceral glomerular epithelial cells (Yang *et al.* 1996; Wharram *et al.* 2000). In addition, the expression of VE-PTP is restricted to endothelial cells and is especially prominent in those of arteries and arterioles (Bäumer *et al.* 2006; Dominguez *et al.* 2007), with VE-PTP also being localized at the apical surface of these cells (Bäumer *et al.* 2006; Dominguez *et al.* 2007). Thus, these observations suggest that the expression of RPTPs of the R3 subtype may be restricted to a single or limited number of cell types. In addition, these RPTPs may be expressed specifically at the apical surface of polarized cells.

In terms of post-translational modification, SAP-1 as well as PTPRO and VE-PTP are highly glycosylated proteins that contain multiple N-glycosylation sites in its extracellular region (Krueger *et al.* 1990; Matozaki *et al.* 1994; Thomas *et al.* 1994). However, it has never been studied whether R3 subtype RPTPs undergo other post-translational modifications. Thus, we have here examined whether these RPTPs could undergo tyrosine phosphorylation or not.

Results

Tyrosine phosphorylation of SAP-1

To examine whether SAP-1 undergoes tyrosine phosphorylation or not, HEK293A cells were transiently transfected with an expression vector for wild-type mouse SAP-1. The cells were thereafter incubated with 100 μM pervanadate, a potent inhibitor for various PTPs, for 10 min, after which the cell lysates were subjected to immunoprecipitation with a monoclonal antibody (mAb) to mouse SAP-1. The immunoblot analysis of the immunoprecipitates with a mAb to phosphotyrosine showed that the treatment of cells with pervanadate markedly promoted tyrosine phosphorylation of SAP-1 (Fig. 1A). Mouse SAP-1 is highly expressed in gastrointestinal epithelial cells (Sadakata *et al.* 2009). Treatment of isolated mouse

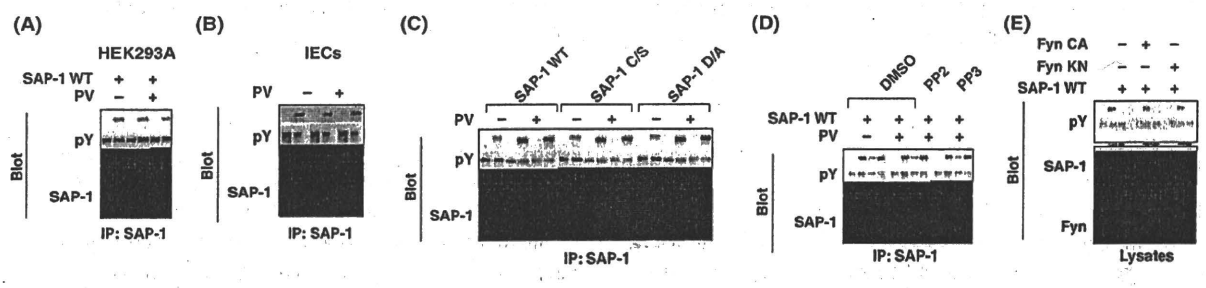

Figure 1 Tyrosine phosphorylation of SAP-1. (A) HEK293A cells were transfected with an expression vector for wild-type SAP-1 (SAP-1 WT). Forty-eight h after transfection, the cells were treated with or without 100 μM pervanadate (PV) for 10 min, after which the cell lysates were prepared and subjected to immunoprecipitation with a mAb to SAP-1. The resulting precipitates were subjected to immunoblot analysis with mAbs to phosphotyrosine (pY) or to SAP-1. (B) Isolated mouse intestinal epithelial cells (IECs) were treated with or without 100 μM pervanadate for 10 min. The cell lysates were then prepared and subjected to immunoprecipitation and immunoblot analysis as in (A). (C) HEK293A cells were transfected with an expression vector for either wild-type SAP-1 (SAP-1 WT), SAP-1 C/S or SAP-1 D/A. Forty-eight h after transfection, the cells were treated with or without 100 μM pervanadate for 10 min, after which the cell lysates were prepared and subjected to immunoprecipitation and immunoblot analysis as in (A). (D) HEK293A cells that had been transfected as in (A) were cultured with DMSO, 10 μM PP2 or 10 μM PP3 for 30 min, after which the cells were treated with or without 100 μM pervanadate for additional 10 min. The cell lysates were then prepared and subjected to immunoprecipitation and immunoblot analysis as in (A). (E) HEK293A cells were transfected with an expression vector for wild-type SAP-1 (SAP-1 WT) together with an empty vector or an expression vector for a catalytically active (CA) form of Fyn or a kinase-negative (KN) form of Fyn. Forty-eight h after transfection, the cell lysates were prepared and subjected to immunoprecipitation and immunoblot analysis as in (A) (upper two panels) or directly to immunoblot analysis with pAbs to Fyn (lower panel). Results in A–E are representative of three independent experiments.

intestinal epithelial cells (IECs) with pervanadate also markedly increased the tyrosine phosphorylation of SAP-1, with low but detectable tyrosine phosphorylation of this protein being observed without pervanadate treatment (Fig. 1B). These results suggest that SAP-1, which is expressed either endogenously or exogenously, undergoes tyrosine phosphorylation upon pervanadate treatment. We next studied the participation of SAP-1 PTP activity in the regulation of tyrosine phosphorylation of SAP-1. To this end, two catalytically inactive mutants of mouse SAP-1, SAP-1 C/S or SAP-1 D/A (Noguchi *et al.* 2001), in which Cys^{871} or Glu^{837} was replaced by Ser or Ala, respectively, were expressed in HEK293A cells and thereafter the cells expressing the mutant SAP-1 were treated with pervanadate. The level of tyrosine phosphorylation of either SAP-1 mutant was markedly greater than that of wild-type SAP-1 in the pervanadate-treated cells (Fig. 1C), suggesting that the PTP activity of SAP-1 negatively regulates tyrosine phosphorylation of this protein.

We next examined whether Src family kinases (SFKs) (Thomas & Brugge 1997) participate in the pervanadate-induced tyrosine phosphorylation of SAP-1. Indeed, treatment of cells with PP2, an inhibitor of SFKs (Hanke *et al.* 1996), but not PP3, an inactive analog of PP2, nor DMSO (vehicle), markedly inhibited the pervanadate-induced tyrosine phosphorylation of SAP-1 in HEK293A cells (Fig. 1D). Furthermore, co-expression of SAP-1 with a catalytically active mutant (Fyn CA) of Fyn, a member of SFKs, but not that with a kinase-inactive mutant of Fyn (Fyn KN), resulted in marked tyrosine phosphorylation of SAP-1 in HEK293A cells (Fig. 1E). Similarly, co-expression of SAP-1 with Src, another member of SFKs, also promoted the tyrosine phosphorylation of SAP-1 in HEK293A cells (data not shown). These results suggest that SFKs participate in the pervanadate-promoted tyrosine phosphorylation of SAP-1.

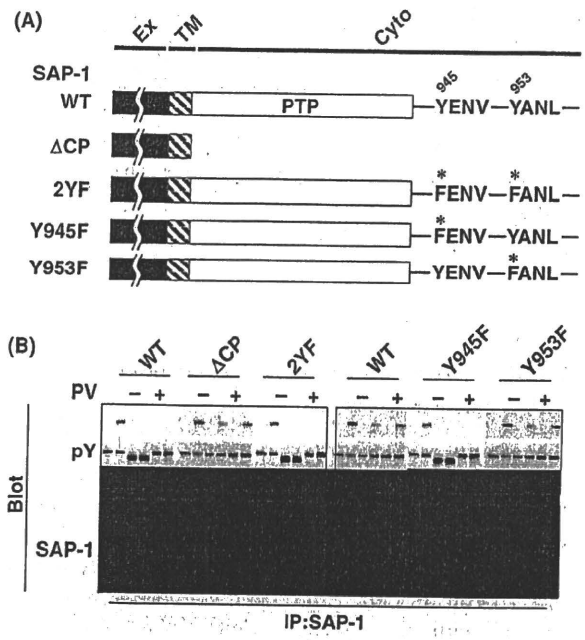

Figure 2 Two tyrosine residues in the COOH-terminus of SAP-1 are important for the pervanadate-promoted tyrosine phosphorylation of SAP-1. (A) Schematic representation of mouse SAP-1. Black, hatched and white boxes indicate the extracellular (Ex), transmembrane (TM) and tyrosine phosphatase (PTP) regions of SAP-1, respectively. Cyto, cytoplasmic region. WT, wild type. Y and F (indicated by asterisks) indicate the positions of tyrosine and phenylalanine, respectively. (B) HEK293A cells were transfected with the vectors for expression of wild type or mutants of SAP-1 as indicated. Forty-eight h after transfection, the cells were treated with or without 100 μM pervanadate (PV) for 10 min. The cell lysates were then prepared and subjected to immunoprecipitation with a mAb to SAP-1, followed by immunoblot analysis with mAbs to phosphotyrosine (pY) or to SAP-1. Results are representative of three independent experiments.

Two tyrosine residues in the COOH-terminus of SAP-1 are important for phosphorylation of SAP-1

We next examined which tyrosine residues of SAP-1 are important for the pervanadate-promoted phosphorylation of SAP-1. The COOH-terminal regions of other PTPs, such as PTPα and PTPε (R4 subtype RPTPs), or SHP-2, a non-receptor type PTP, are known to undergo tyrosine phosphorylation (den Hertog *et al.* 2008). We indeed found that two tyrosine residues, namely Tyr^{945} and Tyr^{953}, for potential phosphorylation sites, are present in the COOH-terminal region of SAP-1 (Fig. 2A). We thus generated expression vectors for various mutants of the cytoplasmic region of SAP-1 as shown in Fig. 2A. HEK293A cells that had been transfected with vectors for SAP-1 mutants were treated with pervanadate, and the extent of tyrosine phosphorylation of each SAP-1 mutant was evaluated. A deletion mutant of SAP-1, ΔCP, which lacked most of the cytoplasmic region of SAP-1, underwent minimal tyrosine phosphorylation in response to the pervanadate treatment (Fig. 2B). Another mutant, 2YF, in which both Tyr^{945} and Tyr^{953} were replaced by Phe, also failed to undergo tyrosine phosphorylation by the pervana-

date treatment (Fig. 2B). Moreover, the extent of the pervanadate-induced tyrosine phosphorylation of either Y945F or Y953F, in which Tyr^{945} and Tyr^{953} were replaced by Phe, respectively, was markedly decreased, compared with that apparent with wild-type SAP-1 (Fig. 2B). Taken together, these results suggest that both Tyr^{945} and Tyr^{953} in the COOH-terminal region of SAP-1 are major sites for the pervanadate-promoted tyrosine phosphorylation of this PTP.

Complex formation of tyrosine-phosphorylated SAP-1 with Grb2 or Fyn

The amino acid sequences surrounding Tyr^{945} and Tyr^{953} of SAP-1 are Y^{945}ENV and Y^{953}ANL, respectively (Fig. 2A). According to the *in vitro* binding studies with a phosphotyrosyl peptide library (Songyang *et al.* 1993, 1994), these amino acid sequences downstream of Tyr^{945} and Tyr^{953} of SAP-1 well correspond with the sequence motif (YxNϕ: ϕ, hydrophobic amino acid; x, any amino acid) for a binding site of the Src homology-2 (SH2) domain of Grb2 or that of the SH2 domains of SFKs. We thus next carried out the pull-down assay to examine whether the SH2 domain of Grb2 could bind to tyrosine-phosphorylated SAP-1. In this assay, we examined the ability of SAP-1 D/A to bind glutathione-S-transferase (GST) fusion proteins containing the SH2 domains of various signaling molecules because the extent of tyrosine phosphorylation of SAP-1 D/A mutant in response to pervanadate treatment was much greater than that of wild-type SAP-1 (Fig. 1C). Either the GST-full-length Grb2 fusion protein or the GST-SH2 domain of Grb2 fusion protein, but not GST alone, precipitated SAP-1 D/A protein from the lysates prepared from pervanadate-treated HEK293A cells that had been transfected with an expression vector for SAP-1 D/A (Fig. 3A). In contrast, these GST fusion proteins failed to precipitate SAP-1 D/A-2YF mutant protein, in which both Tyr^{945} and Tyr^{953} were replaced by Phe, from pervanadate-treated HEK293A cells that had been transfected with an expression vector for SAP-1 D/A-2YF (Fig. 3A). The amino acid sequences downstream of either Tyr^{945} or Tyr^{953} of SAP-1 also correspond to those for the binding site of the SH2 domain of Fes (YExϕ) or Abl (YxNϕ) (Songyang *et al.* 1993, 1994). However, neither GST-SH2 domain of Fes nor GST-SH2 domain of Abl fusion proteins bound the SAP-1 D/A protein from the lysates prepared from pervanadate-treated HEK293A cells (data not shown).

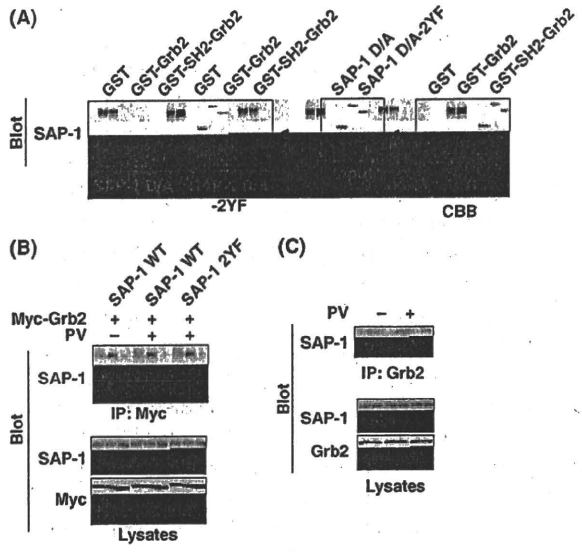

Figure 3 A complex formation of tyrosine-phosphorylated SAP-1 with Grb2. (A) Cell lysates that had been prepared from pervanadate-treated HEK293A cells expressing SAP-1 D/A or SAP-1 D/A-2YF were incubated with GST or GST fusion proteins (GST-Grb2 and GST-SH2-Grb2) immobilized on glutathione-Sepharose beads for 1 h. The beads were washed and the proteins bound to the beads were subjected to immunoblot analysis with a mAb to SAP-1 (left panel). To confirm the amounts of SAP-1 D/A or SAP-1 D/A-2YF in the cell lysates, one-tenth of each cell lysate (Input) used for the pull-down assay was also directly subjected to immunoblot analysis with the same antibody (middle panel). Coomassie Brilliant Blue (CBB) staining also indicates the amounts of GST and GST fusion proteins used in the assay (right panel). (B) HEK293A cells were transiently transfected with expression vectors for wild-type SAP-1 (SAP-1 WT) or SAP-1 2YF together with an expression vector for Myc epitope-tagged Grb2 (Myc-Grb2) and thereafter treated with or without 100 μM pervanadate (PV) for 10 min. The cell lysates were subjected to immunoprecipitation with a mAb to Myc, followed by immunoblot analysis with a mAb to SAP-1 (upper panel). Whole cell lysates (Lysates) were also directly subjected to immunoblot analysis with mAbs to SAP-1 or to Myc (lower two panels). (C) IECs isolated from mouse intestine were treated with or without 100 μM pervanadate for 10 min. The cell lysates were subjected to immunoprecipitation with pAbs to Grb2, followed by immunoblot analysis with a mAb to SAP-1 (upper panel). Whole cell lysates (Lysates) were also directly subjected to immunoblot analysis with a mAb to SAP-1 or pAbs to Grb2 (lower two panels). Results in A–C are representative of three independent experiments.

We next examined whether tyrosine phosphorylation of SAP-1 indeed promotes a complex formation of this PTP with Grb2 in cultured cells. Wild-type SAP-1, but not 2YF mutant, formed a complex with

Myc epitope-tagged Grb2 when both proteins were expressed in HEK293A cells and the cells were thereafter treated with pervanadate (Fig. 3B). SAP-1 was also co-immunoprecipitated with Grb2 from pervanadate-treated isolated mouse IECs, in which both SAP-1 and Grb2 were endogenously expressed (Fig. 3C). Thus, these results suggest that tyrosine phosphorylation of SAP-1 in the COOH-terminal region promotes a complex formation of SAP-1 with Grb2 through the SH2 domain of the latter protein.

We next investigated whether the SH2 domains of SFKs also bind to tyrosine-phosphorylated SAP-1 *in vitro*. Fyn, a member of SFKs, is expressed in various types of cells including gastrointestinal epithelial cells, podocytes, neurons and endothelial cells (Thomas & Brugge 1997). By the pull-down assay, the GST-SH2 domain of Fyn fusion proteins, as well as that of Grb2 fusion proteins (a positive control), precipitated SAP-1 D/A but not SAP-1 D/A-2YF from the lysates of pervanadate-treated HEK293A cells (Fig. 4A). Moreover, wild-type SAP-1 was co-immunoprecipitated with Fyn CA from HEK293A cells that exogenously expressed both proteins, whereas SAP-1 2YF mutant was not (Fig. 4B). These results suggest that tyrosine phosphorylation of SAP-1 in the COOH-terminal region also promotes a complex formation of SAP-1 with Fyn through the SH2 domain of the latter protein.

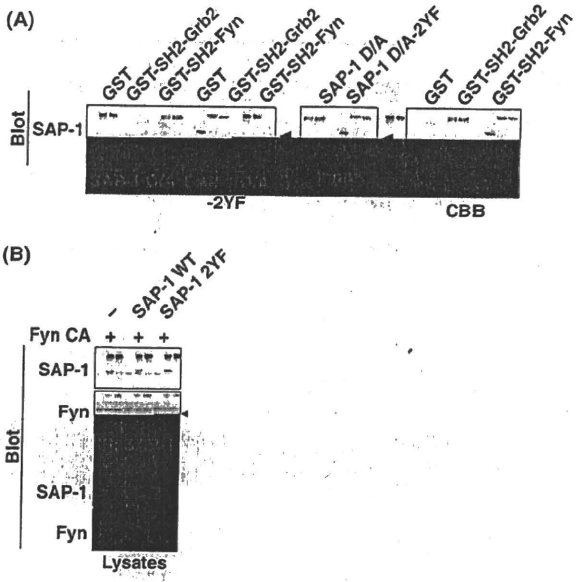

Figure 4 A complex formation of tyrosine-phosphorylated SAP-1 with Fyn. (A) Cell lysates that had been prepared from pervanadate-treated HEK293A cells expressing SAP-1 D/A or SAP-1 D/A-2YF were incubated with GST or GST fusion proteins (GST-SH2-Grb2 and GST-SH2-Fyn) immobilized on glutathione-Sepharose beads for 1 h. The beads were washed and the proteins bound to the beads were subjected to immunoblot analysis with a mAb to SAP-1 (left panel). To confirm the amounts of SAP-1 D/A or SAP-1 D/A-2YF in the cell lysates, one-tenth of each cell lysate (Input) used for the pull-down assay was also directly subjected to immunoblot analysis with the same antibody (middle panel). Coomassie Brilliant Blue (CBB) staining also indicates the amounts of GST and GST fusion proteins used in the assay (right panel). (B) HEK293A cells were transiently transfected with expression vectors for wild-type SAP-1 (SAP-1 WT) or SAP-1 2YF together with an expression vector for a catalytically active Fyn (Fyn CA). The cell lysates were then subjected to immunoprecipitation with a mAb to SAP-1. The resulting precipitates were subjected to immunoblot analysis with a mAb to SAP-1 or pAbs to Fyn (upper two panels). An arrowhead indicates the immunoblot band for Fyn. Whole cell lysates (Lysates) were also directly subjected to immunoblot analysis with the same antibodies (lower two panels). Results in A and B are representative of three independent experiments.

Tyrosine phosphorylation of PTPRO and VE-PTP and their association with Grb2 or Fyn

We found that the COOH-terminal region of either PTPRO or VE-PTP also contains the same amino acid sequence, Tyr-Glu-Asn-Val (YENV), as that of SAP-1 (Y^{945}ENV) (Fig. 5A). We thus next examined whether PTPRO or VE-PTP undergoes tyrosine phosphorylation in their COOH-terminal regions. Indeed, the treatment with pervanadate of wild-type PTPRO- or VE-PTP-expressing HEK293A cells resulted in marked tyrosine phosphorylation of these RPTPs (Fig. 5B). In contrast, the substitution of Tyr^{1220} of PTPRO or Tyr^{1982} of VE-PTP to Phe markedly reduced the tyrosine phosphorylation of mutant RPTP proteins (PTPRO Y1220F or VE-PTP Y1982F, respectively) (Fig. 5B). These results suggest that Tyr^{1220} of PTPRO or Tyr^{1982} of VE-PTP is required for the pervanadate-induced tyrosine phosphorylation of these RPTPs. Expression of Fyn CA together with wild-type PTPRO or VE-PTP promoted the tyrosine phosphorylation of these RPTPs in HEK293A cells (Fig. 5C), suggesting that Fyn is important for tyrosine phosphorylation of both PTPRO and VE-PTP as well as SAP-1.

We next examined whether tyrosine-phosphorylated PTPRO or VE-PTP also binds Grb2 or Fyn via the YxNϕ motif of these RPTPs in cultured cells. Either PTPRO (wild-type or Y1220F mutant) or VE-PTP (wild-type or Y1982F mutant) was

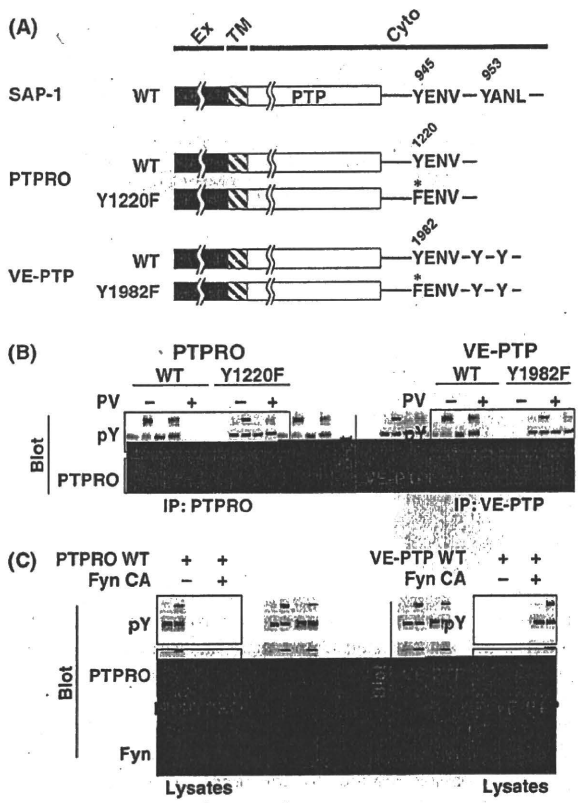

Figure 5 Tyrosine phosphorylation of PTPRO and VE-PTP in their COOH-terminal regions. (A) Schematic representation of R3 subtype RPTP mutants. (B) HEK293A cells were transiently transfected with expression vectors for wild-type PTPRO (PTPRO WT), mutant PTPRO (PTPRO Y1220F), wild-type VE-PTP (VE-PTP WT) or mutant VE-PTP (VE-PTP Y1982F). Forty-eight h after transfection, the cells were treated with or without 100 μM pervanadate (PV) for 10 min. The cell lysates were immunoprecipitated with mAbs to PTPRO (left panels) or to VE-PTP (right panels). The resulting precipitates were subjected to immunoblot analysis with mAbs to phosphotyrosine (pY; left and right upper panels), to PTPRO (left lower panel) or to VE-PTP (right lower panel). (C) HEK293A cells were transfected with expression vectors for wild-type PTPRO (PTPRO WT) or wild-type VE-PTP (VE-PTP WT) together with an empty vector or an expression vector for a catalytically active form of Fyn (Fyn CA). Forty-eight h after transfection, the cell lysates were then subjected to immunoprecipitation with mAbs to PTPRO (left upper and middle panels) or to VE-PTP (right upper and middle panels). The resulting precipitates were subjected to immunoblot analysis with mAbs to phosphotyrosine (pY; left and right upper panels), to PTPRO (left middle panel) or to VE-PTP (right middle panel). Whole cell lysates (Lysates) were also subjected directly to immunoblot analysis with pAbs to Fyn (left and right lower panels). Results in B and C are representative of three independent experiments.

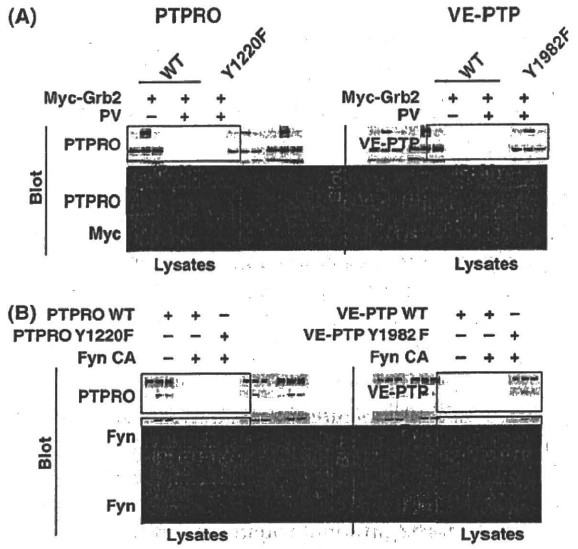

Figure 6 A complex formation of tyrosine-phosphorylated PTPRO or VE-PTP with Grb2 or Fyn. (A) HEK293A cells were transfected with expression vectors for wild-type PTPRO (PTPRO WT), mutant PTPRO (PTPRO Y1220F), wild-type VE-PTP (VE-PTP WT) or mutant VE-PTP (VE-PTP Y1982F) together with an expression vector for Myc epitope-tagged Grb2, after which the cells were treated with or without 100 μM pervanadate (PV) for 10 min. The cell lysates were then subjected to immunoprecipitation with a mAb to Myc (left and right upper panels), followed by immunoblot analysis with mAbs to PTPRO (left upper panel) or to VE-PTP (right upper panel). Whole cell lysates (Lysates) were directly subjected to immunoblot analysis with mAbs to PTPRO (left middle panel), to VE-PTP (right middle panel) or to Myc (left and right lower panels). (B) HEK293A cells were transiently transfected with expression vectors for wild type and mutant PTPRO or VE-PTP as in (A), together with an empty vector or an expression vector for a catalytically active form of Fyn (Fyn CA). The cell lysates were then subjected to immunoprecipitation with mAbs to PTPRO (left upper and middle panels) or to VE-PTP (right upper and middle panels), followed by immunoblot analysis with mAbs to PTPRO (left upper panel), to VE-PTP (right upper panel) or pAbs to Fyn (left and right middle panels). Whole cell lysates (Lysates) were also directly subjected to immunoblot analysis with pAbs to Fyn (left and right lower panels). Results in A and B are representative of three independent experiments.

overexpressed together with Myc epitope-tagged Grb2 in HEK293A cells. Wild-type PTPRO or VE-PTP was co-immunoprecipitated with Grb2 from the cells treated with pervanadate (Fig. 6A). However, association of either PTPRO Y1220F or VE-PTP Y1982F with Grb2 was barely detectable in the pervanadate-treated HEK293A cells (Fig. 6A). Simi-

larly, forced expression of Fyn CA together with wild-type PTPRO or VE-PTP in HEK293A cells resulted in complex formations of these RPTPs with Fyn CA, although the interaction of either PTPRO Y1220F or VE-PTP Y1982F with Fyn CA was minimal (Fig. 6B).

Importance of the YxNϕ motifs of R3 subtype RPTPs for cell spreading and lamellipodium formation

We finally investigated the biological importance of the COOH-terminal YxNϕ motif of SAP-1, PTPRO or VE-PTP. Grb2 is an adaptor protein that forms a complex with a guanine nucleotide exchange protein, Son of sevenless (SOS), that promotes activation of Ras/mitogen-activated protein kinase (MAPK) pathway (Schlessinger & Lemmon 2003). As phosphorylation of the COOH-terminal YxNϕ motifs mediates the association of R3 subtype RPTPs with Grb2, such complex formation might participate in the regulation of the Ras/MAPK pathway. However, forced expression of either wild-type SAP-1 or SAP-1 2YF failed to affect the epidermal growth factor (EGF)-stimulated activation of MAPK in COS7 cells (data not shown), suggesting that the COOH-terminal YxNϕ motif of SAP-1 is unlikely important for regulation of the EGF-stimulated Ras/MAPK activation.

We have recently found that forced expression of VE-PTP promotes cell spreading as well as formation of lamellipodia and filopodia in cultured fibroblasts plated on fibronectin (Mori *et al.* 2010). These effects of VE-PTP on cell morphology require its catalytic activity as well as activation of SFKs. Moreover, forced expression of VE-PTP increased the activity of Src (Mori *et al.* 2010). We thus next investigated whether the COOH-terminal YxNϕ motif is important for the R3 subtype RPTPs-induced cell morphological changes. Indeed, forced expression of SAP-1 or that of PTPRO also promoted cell spreading and formation of lamellipodia and filopodia in Chinese hamster ovary (CHO) cells that expressed an active form of H-Ras (CHO-Ras cells) (Fig. 7A,B). In contrast, the effect of forced expression of either VE-PTP Y1982F, SAP-1 2YF or PTPRO Y1220F on cell spreading and lamellipodium formation in CHO-Ras cells tended to be smaller than that of each corresponding wild-type RPTP (Fig. 7C). Quantitative analysis showed that the effect of VE-PTP Y1982F or PTPRO Y1220F on lamellipodium formation was indeed smaller than that of wild-type PTPRO or VE-PTP, and the effect of SAP-1 2YF also tended to be smaller than that of wild-type SAP-1, although this difference was not statistically significant (Fig. 7D). These data suggest that the COOH-terminal YxNϕ motif of VE-PTP, SAP-1 or PTPRO is important for regulation by these RPTPs of cell morphology.

Discussion

We here show that R3 subtype RPTPs, such as SAP-1, PTPRO and VE-PTP, share the same amino acid motif (YxNϕ) in their COOH-terminal regions. Moreover, these YxNϕ motifs undergo tyrosine phosphorylation by pervanadate treatment of cells. DEP-1 is also a family member of R3 subtype RPTPs. We found that YxNϕ motifs (Y^{1221}ENL for mouse DEP-1) are present in the COOH-terminal regions of mouse, rat and human DEP-1. Thus, DEP-1 likely undergoes tyrosine phosphorylation in the COOH-terminal region. The regulatory mechanism for the tyrosine phosphorylation of R3 subtype RPTPs was also investigated in this study. Inhibition by PP2 of SFKs abolished the pervanadate-induced tyrosine phosphorylation of SAP-1. In addition, forced expression of Fyn (or Src) markedly induced tyrosine phosphorylation of SAP-1 as well as PTPRO and VE-PTP. Thus, SFKs are likely important for tyrosine phosphorylation of these RPTPs. In contrast, activation of growth factor receptors, such as insulin- or EGF-receptors, failed to promote tyrosine phosphorylation of SAP-1 in CHO cells overexpressing SAP-1 and either insulin- or EGF-receptors (Y. Murata and T. Matozaki, unpublished data), suggesting that these receptor tyrosine kinases may not be important for tyrosine phosphorylation of R3 subtype RPTPs. However, it is recently shown that DEP-1 undergoes tyrosine phosphorylation in response to EGF in HeLa cells (Tarcic *et al.* 2009). Given that the level of pervanadate-induced tyrosine phosphorylation of a catalytically inactive mutant of SAP-1 (either SAP-1 C/S or SAP-1 D/A) was markedly greater than that of wild-type SAP-1, the COOH-terminal phosphorylated YxNϕ motif is likely regulated by auto-dephosphorylation by SAP-1.

We also showed that the phosphorylation of SAP-1, PTPRO or VE-PTP at the YxNϕ motif promotes complex formations of these RPTPs with Grb2 or Fyn likely through the SH2 domain of Grb2 or of Fyn. These results indicate that R3 subtype RPTPs function as not only PTPs but also as docking proteins for SH2 domain-containing

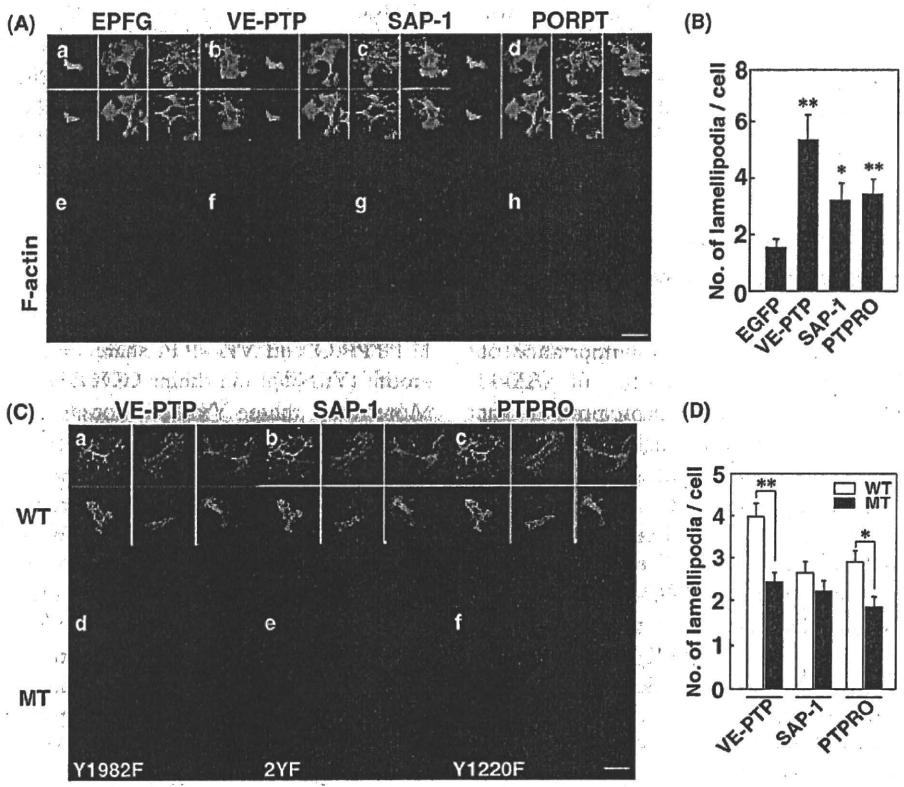

Figure 7 Importance of the COOH-terminal YxNϕ motifs of R3 subtype RPTPs for cell spreading and lamellipodium formation induced by R3 subtype RPTPs. (A) CHO-Ras cells were transiently transfected with expression vectors for EGFP (a, e), wild-type VE-PTP (VE-PTP; b, f), wild-type SAP-1 (SAP-1; c, g) or wild-type PTPRO (PTPRO; d, h). Twenty-four h after transfection, the cells were deprived of serum for 8 h, replated on cover glasses coated with fibronectin (20 μg/mL) and cultured in serum-free medium for additional 2 h. The cells were then fixed, stained with rhodamine-conjugated phalloidin (e–h) to visualize F-actin, and either immunostained with mAbs to VE-PTP (b), SAP-1 (c) or to PTPRO (d) or monitored for EGFP fluorescence (a). Bar, 20 μm. (B) CHO-Ras cells transfected and treated as in (A) were evaluated for the number of lamellipodia as described in Experimental procedures. Data are means ± SE from 20 cells for each condition and are representative of three independent experiments. $*P < 0.05$, $**P < 0.01$ (ANOVA and Bonferroni's test) versus the corresponding value for EGFP-expressing cells. (C) CHO-Ras cells were transiently transfected with expression vectors for wild type (WT) R3 subtype RPTPs [VE-PTP (a), SAP-1 (b) and PTPRO (c)], or a non-tyrosine-phosphorylated mutant (MT) of R3 subtype RPTPs [VE-PTP Y1980F (d), SAP-1 2YF (e) and PTPRO Y1220F (f)]. Twenty-four h after transfection, the cells were fixed and immunostained with mAbs to VE-PTP (a, d), to SAP-1 (b, e) or PTPRO (c, f). Bar, 20 μm. (D) CHO-Ras cells were transfected as in (C) and thereafter treated as in (A). The number of lamellipodia per transfected cell (identified by SAP-1, PTPRO or VE-PTP immunofluorescence) was determined. Data are means ± SE from a total of 80 cells for each condition in three independent experiments. $*P < 0.05$, $**P < 0.01$ (Student's *t* test). Results in A and C are representative of three independent experiments.

signaling molecules. However, the functional significance for the binding of Grb2 to R3 subtype RPTPs remains unclear. Grb2 is implicated in regulation of clathrin-mediated endocytosis of EGF receptors by the interaction of Grb2 via its SH2 domain with EGF receptors (Sorkin 2004). Thus, interaction of tyrosine-phosphorylated R3 subtype RPTPs with Grb2 might participate in regulation of endocytosis of these RPTPs.

On the contrary, the complex formation of SAP-1, PTPRO or VE-PTP with Fyn or other SFKs might be important for regulation of the SFK activity. It was previously shown that R4 subtype RPTPs (Andersen *et al.* 2001), such as PTPα and PTPε, also undergo tyrosine phosphorylation of their COOH-terminal regions (Pallen 2003; Berman-Golan & Elson 2007). Moreover, tyrosine phosphorylation of these RPTPs promotes binding of these RPTPs

to the SH2 domain of Src. This binding results in disruption of the closed conformation formed by interaction between the SH2 domain and the COOH-terminal phosphorylated Tyr^{527} of Src. Consequently, the phosphorylated Tyr^{527} is exposed to and dephosphorylated by PTPα or PTPε, leading to activation of Src. Thus, it is possible that tyrosine phosphorylation of SAP-1, PTPRO or VE-PTP promotes their binding of SFKs, resulting in activation of SFKs in a manner similar to PTPα or PTPε. Indeed, we have recently shown that forced expression of VE-PTP indeed increases the activity of Src (Mori *et al.* 2010).

We also showed that forced expression of wild-type VE-PTP, SAP-1 or PTPRO promoted lamellipodium formation in CHO-Ras cells. In contrast, the effect of forced expression of VE-PTP Y1982F or PTPRO Y1220F on lamellipodium formation was markedly smaller than those of wild-type RPTPs, and the effect of SAP-1 2YF also tended to be smaller than that of wild-type SAP-1. The effect of forced expression of VE-PTP on lamellipodium formation is thought to require the activities of SFKs (Mori *et al.* 2010). Taken together, it is likely that the phosphorylation of the COOH-terminal YxNϕ motifs of R3 subtype RPTPs promotes the binding of these RPTPs with SFKs and subsequent activation of SFKs. Such complex formation might be important for the regulation by R3 subtype RPTPs of cell morphology. The effect of VE-PTP on lamellipodium formation was much greater than that of SAP-1 or PTPRO, suggesting a notion that VE-PTP can activate SFKs better than the latter two RPTPs. In addition, the effects of wild-type SAP-1 and SAP-1 2YF on lamellipodium formation were not markedly different. Thus, forced expression of SAP-1 might promote lamellipodium formation through a pathway dependent on or independent of tyrosine phosphorylation of this RPTP.

Experimental procedures

Antibodies and reagents

Rat mAbs to mouse SAP-1, to mouse PTPRO or to mouse VE-PTP were generated and prepared as previously described (Kotani *et al.* 2009; Sadakata *et al.* 2009; Mori *et al.* 2010). A mouse mAb to phosphotyrosine (4G10) was from Millipore (Billerica, MA, USA). A mouse mAb to the Myc epitope tag (9E10) was purified from the culture supernatants of hybridoma cells. Rabbit polyclonal antibodies (pAbs) to Grb2 or to Fyn were from Santa Cruz Biotechnology (Santa Cruz, CA, USA). Horseradish peroxidase-conjugated goat pAbs to rabbit, mouse or rat IgG were from Jackson ImmunoResearch (West Grove, PA, USA). Rhodamine-conjugated phalloidin and Alexa488-conjugated goat pAbs to rat IgG were from Invitrogen (Carlsbad, CA, USA). PP2 and PP3 were from EMD Chemicals Inc. (Darmstadt, Germany). Fibronectin was from Sigma (Saint Louis, MO, USA).

Plasmids

Expression vectors for mouse SAP-1, mouse VE-PTP and mouse PTPRO were generated as described (Kotani *et al.* 2009; Sadakata *et al.* 2009; Mori *et al.* 2010). A full-length cDNA of mouse Grb2 was amplified by reverse transcription-polymerase chain reaction (RT-PCR) with total RNA from mouse brain (C57BL/6) to construct an expression vector for Myc epitope-tagged Grb2. The resulting polymerase chain reaction (PCR) products for Grb2 were subcloned into pCI-neo-Myc [kindly provided by Y. Takai (Kobe University, Kobe, Japan)]. For expression of enhanced green fluorescent protein (EGFP), the pEGFP-N3 vector was obtained from Clontech (Palo Alto, CA, USA). Expression vectors for an active mutant of mouse Fyn (Fyn CA) and for a kinase-inactive mutant of mouse Fyn (Fyn KN) were kindly provided by T. Yagi (Osaka University, Osaka, Japan). For construction of phosphatase-inactive mutants of SAP-1, cDNAs encoding a catalytically inactive mutant of SAP-1 (SAP-1 C/S), in which Cys^{871} was replaced by Ser, and another catalytically inactive mutant of SAP-1 (SAP-1 D/A), in which Asp^{837} was replaced by Ala, were generated by site-directed mutagenesis with the use of wild-type mouse SAP-1 cDNA as a template and the QuikChange Site-Directed Mutagenesis Kit (Stratagene, La Jolla, CA, USA). The resulting cDNAs were subcloned into pcDNA3.1 (Invitrogen). To construct an expression vector for a mutant of SAP-1, SAP-1 ΔCP, which lacked most of the cytoplasmic region of SAP-1, DNA fragments corresponding to amino acids 1-669 of mouse SAP-1 were amplified by PCR and subcloned into pcDNA3.1. The expression vectors for SAP-1-2YF, -Y945F and -Y953F, in which two tyrosine residues (Tyr^{945} and Tyr^{953}) or either one were replaced by Phe, respectively, were constructed by PCR-ligation-PCR mutagenesis (Ali & Steinkasserer 1995). Expression vectors for PTPRO Y1220F or VE-PTP Y1982F, in which Tyr^{1220} for PTPRO or Tyr^{1982} for VE-PTP was replaced by Phe, respectively, were also constructed by PCR-ligation-PCR mutagenesis. The resulting PCR products were subcloned into pcDNA3.1 (for the SAP-1 mutants and the PTPRO mutant) or pTracer-CMV (for the VE-PTP mutant). Construction of an expression vector for GST-Grb2 was previously described (Sakaue *et al.* 1995). To construct expression vectors for GST-SH2-Grb2, GST-SH2-Fyn, GST-SH2-Fes or GST-SH2-Abl, cDNA fragments corresponding to the SH2 domain of mouse Grb2 (aa 54-164), mouse Fyn (aa 143-247), mouse Fes (aa 448-548) or mouse Abl (aa 140-248) were amplified by RT-PCR as described previously and were then subcloned